

### Characteristics of the ZMP for the biped robot

Chan-Soo Park, and Chong-Ho Choi

Department of Electrical Engineering, Seoul National University, Seoul, Korea  
(Tel : +82-2-880-7310; E-mail: chchoi@csl.snu.ac.kr)

**Abstract:** This is a preliminary study is to make the robot walk more stably by observing the ZMP (Zero Moment Point) of the robot when the robot stands on one leg(single support) and then on two legs(double support) and so on. The robot consists of nine DOF (Degree of freedom) with lower part of the body. It is equipped with motor drivers and force sensors inside the robot. The motors are controlled by the external PC (Intel pentium 4). By the experimental results, it is found that the robot is unstable in the instant of changing from single support to double support or from double support to single support. We use the trajectory compensation of the angle and the length of both legs to realize more stable walking.

**Keywords:** ZMP, biped robot, FSR.

#### 1. INTRODUCTION

Over the past thirty years, many studies have been made on biped walking robots. In 1973, the first biped humanoid robot, WABOT-1, was developed by Kato and others [1]. Up to the present, many biped robots have been developed, but it is not easy to design a practical humanoid robot. Some practical humanoid robot studies are in progress [2-5]. It needs to walk, think, and react like a human. And many related issues such as vision, dynamic analysis, robot design and application, artificial intelligence and minimizing energy consumption have been studied.

Among these issues, we focus on the stability of the walking robot in this paper. Zheng et al. reported the method of gait synthesis for static stability [6]. The methods of ensuring the dynamic stability based on ZMP (Zero Moment Position) have been also studied [7-8]. The ZMP is defined as the point on the ground which the sum of all the moments of the active force is equal to zero. It is desirable that the desired trajectory of ZMP is designed to stay near the center of the stable region of ZMP [9]. This stability should be insured when the robot is walking. To determine the stability, we measured the ZMP with force sensors. If the ZMP is within the convex hull of all contact points between the feet and the ground, it is possible for the biped robot to walk in stable condition. To find a more stable ZMP trajectory, we adjusted the parameters, such as the length of the leg, the angle between the sole and the ground, the weight position and the velocity of each joint.

This paper organized as follows. In section 2, measurement of the ZMP is described. In section 3, experiments on the ZMP trajectory compensation are described. The conclusion follows in section 4.

#### 2. ZMP MEASUREMENT

To measure the force on the sole, total eighteen FSR (Force Sensing Resistor) [10] are equipped on the sole as shown in Fig. 1. The advantages of the FSR are low cost, thin, light and easy to measure. The FSR circuit is made with the op-amp voltage amplifier.

From Eqs. (1) and (2), we calculate the ZMP with the force data on the sole [11].

$$x_{ZMP} = \frac{\sum_{i=1}^n f_i \cdot x_i}{\sum_{i=1}^n f_i} \tag{1}$$

$$y_{ZMP} = \frac{\sum_{i=1}^n f_i \cdot y_i}{\sum_{i=1}^n f_i} \tag{2}$$

Here,  $(x_i, y_i)$  denotes the point on Fig. 1 where the i'th sensor is located, and n is the total number of force sensors.  $f_i$  is the value measured by the i'th sensor. We applied a known force to each FSR and compare the ZMP calculated with Eqs. (1) and (2). There were some discrepancies between the two values and we compensated the ZMP by Fig. 2.

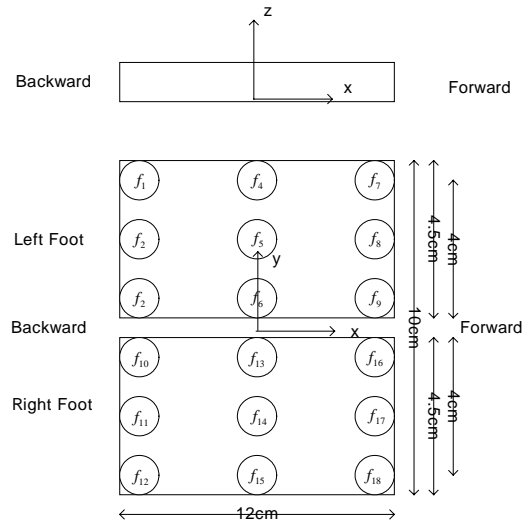


Fig. 1 The positions of FSRs on a sole

The relationship between  $ZMP_{measured}$  and  $ZMP_{compensated}$  in Fig. 2 is

- i)  $y_{ZMP,measured} \leq -2.68$  ;  
 $y_{ZMP,compensated} = y_{ZMP,measured} \times 0.379 - 2.984$  ;
- ii)  $-2.68 < y_{ZMP,measured} \leq 2.68$  ;  
 $y_{ZMP,compensated} = y_{ZMP,measured} \times 1.493$  ;
- iii)  $2.68 < y_{ZMP,measured}$  ;  
 $y_{ZMP,compensated} = y_{ZMP,measured} \times 0.379 + 2.984$  .

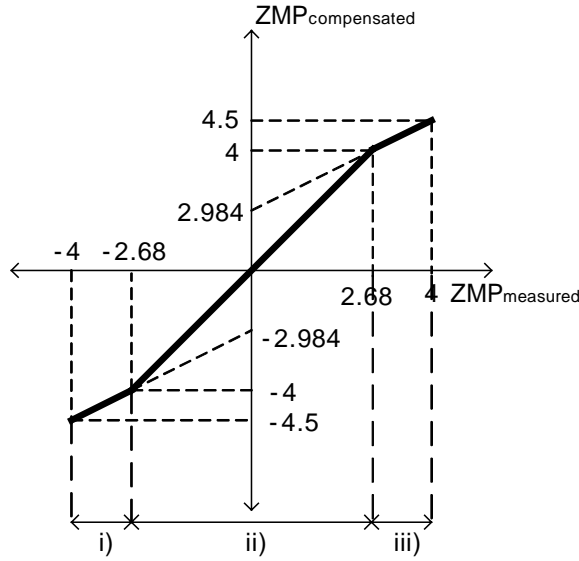


Fig. 2 ZMP compensation

3. EXPERIMENTS

The structure of the robot is shown in Fig. 3. Here, O denotes the origin of the axis. The biped walking robot we used in this experiment is about 45cm tall, 30cm wide and 12cm deep. The total weight is about 4kg including the 1.4kg weight equipped at the midpoint of the hip. The weight moves from right to left or in the opposite directions to make the ZMP stay inside a sole. The advantage of this method using the weight equipped at the midpoint of the hip is that the COM (center of mass) trajectory can be easily divided into two directions, left-right direction and front-rear direction.

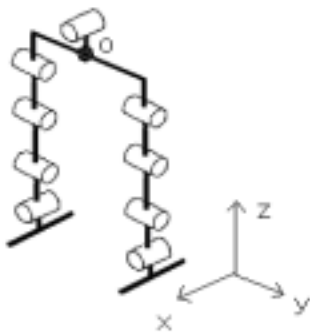


Fig. 3 The structure of the robot

We generate a static walking trajectory and observe the ZMP trajectory when the robot is walking at the same plane, i.e., at the zero velocity. Figure 4 shows the weight trajectory in the y axis. The weight position  $w(t)$  in Fig. 4 is

$$\begin{aligned}
 & \text{i) } nT + t_0 \leq t < nT + t_1 \\
 & w(t) = w_0, \\
 & \text{ii) } nT + t_1 \leq t < nT + t_2 \\
 & w(t) = w_0 \cdot \cos\left\{\left(\frac{t-t_1}{t_2-t_1}\right)\pi\right\}, \\
 & \text{iii) } nT + t_2 \leq t < nT + t_3 \\
 & w(t) = -w_0, \\
 & \text{iv) } nT + t_3 \leq t < nT + t_4 \\
 & w(t) = -w_0 \cdot \cos\left\{\left(\frac{t-t_3}{t_4-t_3}\right)\pi\right\},
 \end{aligned} \tag{1}$$

Here, T denotes one walking period that both leg move up and down one after another and  $T = t_4 - t_0$ . In Eq. (1),  $w(t)$  is in proportion to a cosine function when it moves from one side to another. The weight moves at the maximum speed when it is at the center of the hip.

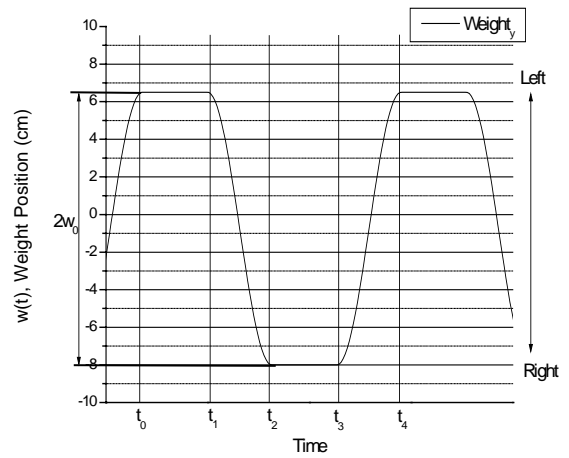


Fig. 4 The weight trajectory in the y axis

Figure 5 shows the sole trajectory in the z axis. The maximum heights which the sole is located from the ground are 2.5cm in the case of right foot and 5cm in the case of left foot. It was found out that the difference in the maximum height between the right and the left sole has little effect on the ZMP for the given trajectory. When the sole leaves or touches the ground, it moves very slowly to reduce the ZMP overshoot as can be seen in Fig. 5.

The walking cycle is divided into the double support phase and the single support phase. In the double support phase, both sole contact the ground. And the weight located at the center of hip moves either from the right to the left or from the left to the right in this phase. In the single support phase, the sole leaves the ground and the leg moves upwards, after a while, moves downwards. The phase terminates when the sole becomes flat with the ground just before it touches the ground.

During the single support phase, one leg is in the support phase, while the other leg is in the swing phase [12].

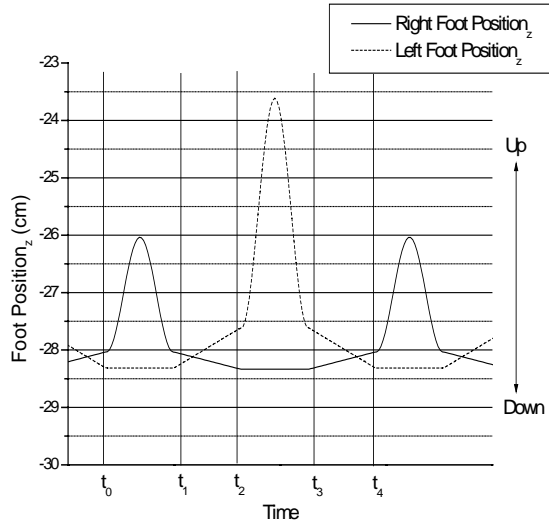


Fig. 5 The sole trajectory in the z axis

Figure 6 shows the ZMP trajectory on the y-axis when the robot is walking at the same plane. Because the sole is longer in the x axis, the robot falls down more easily toward right or left direction than front or rear direction. So only the ZMP trajectory in the y axis is displayed in Fig. 6. One cycle of motion is 62 seconds.

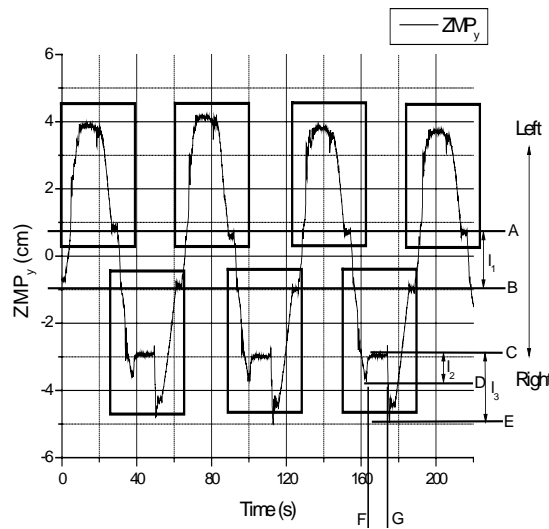


Fig. 6 the ZMP trajectory in the y axis when the robot is walking

In Fig. 6, A(B) denotes the position of the ZMP when the weight moves from the left(right) side to the center of the hip. C denotes the position of the ZMP just after the left sole leaves the ground. D denotes the position of the ZMP just before the left sole leaves the ground. E denotes the position of the ZMP when the left sole contacts the ground. Note that  $l_1 = |A - B|$ ,

$l_2 = |D - C|$ ,  $l_3 = |E - C|$ . We will call  $l_3$  the overshoot of the ZMP.

During the single support phase by the left leg, there are no overshoots in the ZMP when the right sole leaves the ground or contacts with the ground in Fig. 6. But in the case of the single support phase with the right leg, there are overshoots of 2cm. These overshoots have bad effects on the stability of the walking robot. The difference between the ZMP trajectories are conjectured due to some minor differences between the right and the left legs.

So we need to adjust some parameters of the robot to reduce the impact when the sole contacts or leaves the ground.

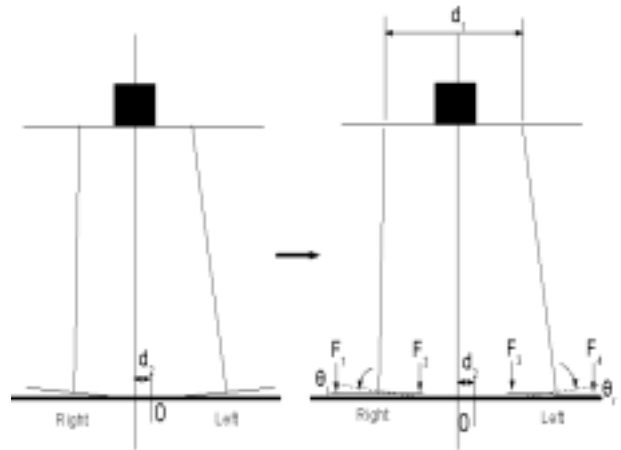


Fig. 7 Ankle compensation with force data  $F_i$ 's

The angles of ankles  $\theta_r$  and  $\theta_l$  in Fig. 7 is 2~3 degree and we need to adjust so that the surface of each sole is paralleled to the ground at the time of contact. To do this, we need to make  $F_1 = F_2$  and  $F_3 = F_4$ , in Fig. 7. Here,  $F_1$  ( $F_2$ ) is the total force measured by the FSR's on the right(left) side of the right sole.  $F_3$  ( $F_4$ ) is the total force measured by the FSR's on the right(left) side of the left sole.

To find out the compensation angle  $\Delta\theta_r$  and  $\Delta\theta_l$  of the ankles, we define the object function as Eq. (3).

$$J_1(\theta_l, \theta_r) = \min\{|F_1(\theta_l, \theta_r) - F_2(\theta_l, \theta_r)| + |F_3(\theta_l, \theta_r) - F_4(\theta_l, \theta_r)|\} \quad (3)$$

If the difference between  $F_1$  and  $F_2$  ( $F_3$  and  $F_4$ ) is sufficiently small, the surface of the right(left) sole becomes paralleled to the ground. To find out  $\Delta\theta_r$  and  $\Delta\theta_l$ , we use the gradient method such as

$$\theta_l(n+1) = \theta_l(n) + \alpha_1 \cdot \frac{\Delta J_1(\theta_l(n), \theta_r(n))}{\Delta \theta_l(n)}$$

$$\theta_r(n+1) = \theta_r(n) + \alpha_2 \cdot \frac{\Delta J_1(\theta_l(n), \theta_r(n))}{\Delta \theta_r(n)}$$

where  $\Delta\theta_l(n) = \theta_l(n) - \theta_l(n-1)$ ,  $\Delta\theta_r(n) = \theta_r(n) - \theta_r(n-1)$ ,  $\Delta J_1(\theta_l(n), \theta_r(n)) = J_1(\theta_l(n), \theta_r(n)) - J_1(\theta_l(n-1), \theta_r(n-1))$ .

Another parameter to adjust is the angle  $\theta$  in fig. 8.

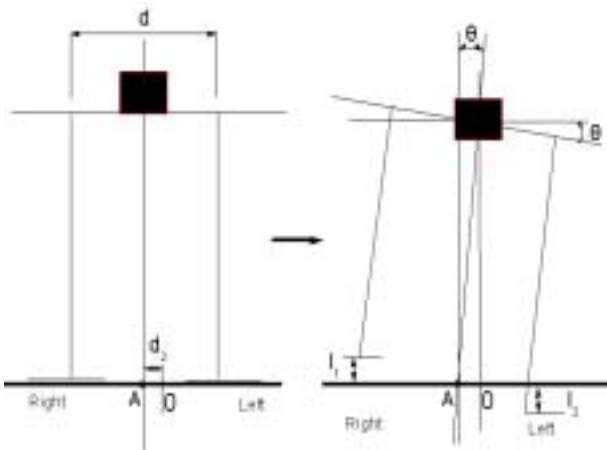


Fig. 8 COM position compensation

In Fig. 8,  $d$  is the length between the left leg and the right leg,  $O$  is the middle point of the soles on the ground,  $A$  is the position of the center of mass (COM) projected on the ground, and  $d_2$  is the distance between  $A$  and  $O$ . The COM of the robot lean toward the right side as shown in Fig. 8. To make the COM of the robot lie on the center of the both soles, we need to tilt the hip by  $\theta$ . To do this, the right leg should be longer by  $l_1$  and the left leg should be shorter by  $l_2$ . We can find out the value  $\theta$  by experiment. Note that  $l_1$  and  $l_2$  are  $l_1 = l_2 = \frac{1}{2} \cdot d \cdot \tan \theta$ .

Figure 9 shows the ZMP trajectory after applying the compensations in Fig. 7 and Fig. 8. In comparison with the ZMP trajectory in Fig. 6, the trajectory in Fig. 9 is more symmetric and the overshoots are decreased.

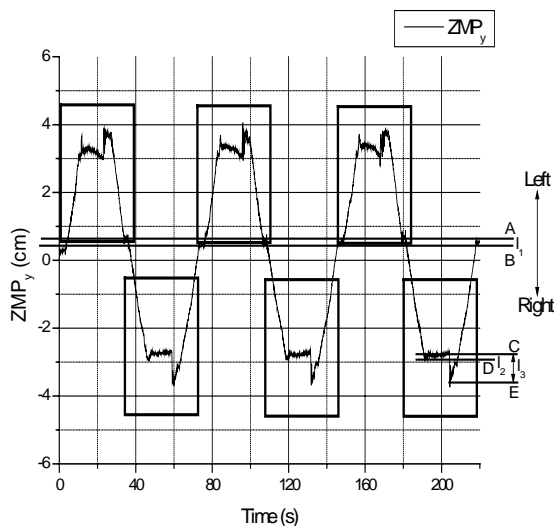


Fig. 9 The ZMP trajectory in the y axis after the compensations

The ZMP trajectory in Fig. 9 is better in repeatability which implies that the walking is more stable. Table 1 shows the result of Fig. 6 and Fig. 9.

It shows that the overshoot  $l_3$  as the sole contacts the ground is decreased to 60%. And  $l_1$  and  $l_2$  are also decreased. After these compensations, the motion of the robot becomes more stable.

Table 1 The parameters comparison between the Fig. 4 and the Fig. 7

	A	B	C	D	E	$l_1$	$l_2$	$l_3$
Fig.4	7.5	-9.5	-28.6	-37.9	-49.3	17	9.3	20.7
Fig.7	6.0	4.2	-27.6	-29.3	-36.0	1.8	1.7	8.4

We also investigated the effect of weight position from the middle of the hip when the sole contacts the ground to the overshoot of the ZMP, which is shown in Fig. 10. If the weight position is further from the middle of the hip, the overshoot of the ZMP decreases. This shows that it is better to move the weight to the side farther to decrease the overshoot of the ZMP.

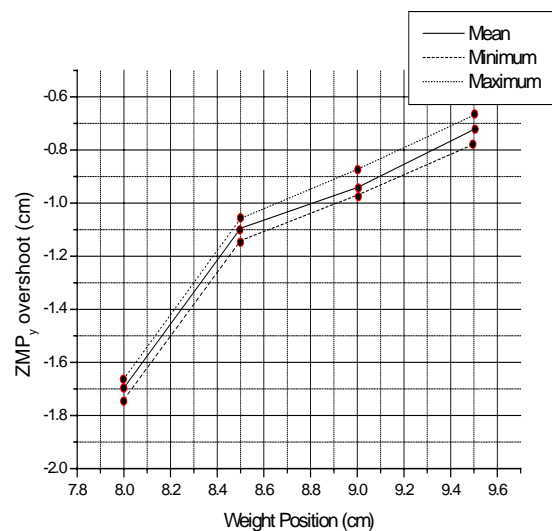


Fig. 10 Weight position vs. the overshoot of the ZMP when the sole contacts the ground

Figure 11 shows the effect on the overshoot of the ZMP by the velocity of the ole in the z-direction. Here,  $v_{sole}$  denotes the maximum velocity when it moves after leaving the ground. The figure shows that the velocity at contact has more effect to the overshoot than  $v_{sole}$ .

Based on these experiments, we generate a faster walking trajectory, i.e.,  $t_0=1s$ ,  $t_1=2.5s$ ,  $t_2=4.2s$ ,  $t_3=5.7s$ ,  $t_4=7.4s$ ,  $T=6.4s$ , and  $w_0=7.25cm$  in Fig. 4 and Fig. 5.

Figure 12 shows the ZMP trajectory for the fast trajectory. It shows good repeatability and stable motion of walking at the same plane.

REFERENCES

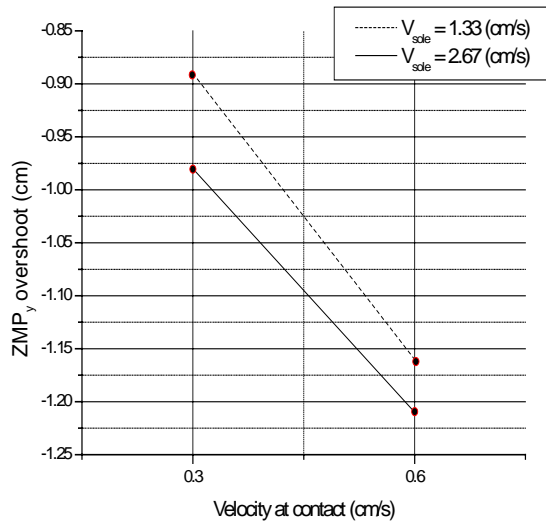


Fig. 11 Sole velocity vs. the ZMP overshoot when the sole contacts the ground

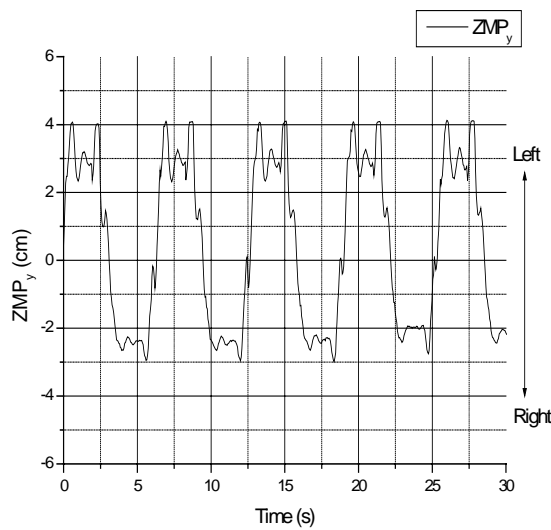


Fig. 12 The ZMP trajectory along the y axis as the walking period is 6.4(s)

4. CONCLUSION

We carried out the experiment with 9 DOF biped walking robot and measured the ZMP with the force sensor. By adjusting the parameters such as the leg lengths, the angles between the sole and the ground, and the weight position, we observed the overshoots of the ZMP decreased. By using the insight obtained in this experiment, we are working for the trajectory design of the robot that walks faster and more naturally.

- [1] I. Kato, "Development of WABOT-1," Biomechanism 2, The University of Tokyo Press, pp. 173-214, 1973(In Japanese).
- [2] H. Miura and I. Shimoyama, "Dynamic walk of a biped" Int. J. of Robotics Research, vol. 3, no. 2, pp.60-74, 1984.
- [3] N. Wagner, M. C. Mulder, and M. S. Hsu, "A Knowledge based control strategy for a biped" Proc. 1988 IEEE Int. Conf. on Robotics and Automation, pp. 1520-1524, April 24-29, 1988.
- [4] Y. F. Zheng and F. Sias, "Design and motion control of practical biped robots" Int. J. of Robotics and Automation, vol. 3, no. 2, pp. 70-78, 1988.
- [5] K. Hirai "Current and Future Perspective of Honda Humanoid Robot" In Proc. of the IEEE/RSJ Int. Conf. on Intelligent Robots and Systems, pp. 500-508, 1997
- [6] Y. F. Zheng and J. Shen, "Gait synthesis for the SD-2 biped robot to climb sloping surface" IEEE trans. Robot. Automat., vol. 6, pp. 86-96, Feb. 1990.
- [7] A. Takanishi, M. Ishida, Y. Yamazaki, and I. Kato, "The realization of dynamic walking robot WL-10RD" in Proc. Int. Conf. Advanced Robotics, pp. 459-466, 1985.
- [8] K. Hirai, M. Hirose, Y. Haikawa, and T. Takenaka, "The development of honda humanoid robot" in Proc. IEEE Int. Conf. Robotics and Automation, pp. 1321-1326, 1998.
- [9] Qiang Huang, Kazuhito Yokoi, Shuuji Kajita, Kenji Kaneko, Hirohiko Arai, Noriho Koyachi, and Kazuo Tanie, "Planning Walking Patterns for a Biped Robot" IEEE Trajsactions on Robotics and Automation, vol. 17, no. 3, pp280-289, June 2001.
- [10] Force Sensing Resistor Informations at the Interlink Electronics website : <http://www.fsrlink.com/>
- [11] Atsushi Konno, Noriyoshi Kato, Satoshi Shirata, Tomoyuki Furuta, "Development of a Light-Weight Biped Humanoid Robot" In Proc. of the IEEE/RSJ Int. Conf. on Intelligent Robots and Systems, pp.1565-1570, 2000
- [12] C.L. Shih, Y. Z. Li, S. Churng, T. T. Lee, W. A. Gruver, "Trajectory Synthesis and Physical Admissibility for a Biped Robot During the Single-Support Phase" in Proc. IEEE Int. Conf. on Robotics and Automation, pp 1646-1652, vol. 3, May 1990.